Biomedicine & Pharmacotherapy 121 (2020) 109612

Contents lists available at ScienceDirect

Biomedicine & Pharmacotherapy

journal homepage: www.elsevier.com/locate/biopha

Effect of an aqueous extract of *Averrhoa carambola* L. on endothelial function in rats with ventricular remodelling

Xingmei Liang[a], Renbin Huang[b], Jianchun Huang[b], Chunxia Chen[b], Feizhang Qin[b], Antao Liu[a], Xiaojun Tang[a], Tian Ning[a], Huiliang Nong[c,*]

[a] Guangxi Medical College, Nanning 530023, Guangxi, P.R. China
[b] Pharmaceutical College, Guangxi Medical University, Nanning 530021, Guangxi, P.R. China
[c] PhaseI Clinical Center, The First People's Hospital of Nanning, Nanning 530022, Guangxi, P.R. China

ARTICLE INFO

Keywords:
AEA
Ventricular remodelling
Endothelial function
Isoprenaline

ABSTRACT

Ventricular remodelling leads to cardiomyocyte hypertrophy, myocardial fibrosis, endothelial vasoactive substance changes and endothelial dysfunction. Our purpose was to research the effect of an aqueous extract of *Averrhoa carambola* L. (AEA) on endothelial function in rats with ventricular remodelling induced by isoprenaline. Rats were subjected to injection of isoprenaline and administration of various drugs. Vasoactive substances were measured, and the ventricular remodelling index was detected by the weighing method. Immunohistochemical analysis, pathological examination, Western blot and Masson's trichrome staining were performed. After AEA administration, the levels of transforming growth factor-β (TGF-β), angiotensin II (AngII), inducible NO synthase (iNOS), endothelin-converting enzyme (ECE), and endothelin 1 (ET-1); the ventricular remodelling index; and the collagen volume fraction were decreased, while the levels of total NO synthase (tNOS) and endothelial NO synthase (eNOS) were increased. The pathological examination results showed that apoptosis, fibrosis, necrosis and inflammatory infiltration of myocardial tissue were attenuated by AEA treatment. AEA might alleviate ventricular remodelling in rats by maintaining the balance of vasoactive substances and the function of the vascular endothelium.

1. Introduction

Ventricular remodelling (VR) results from a compensatory adaptation of the ventricle to a long-term stimulus, such as hypertension, myocardial infarction, myocarditis, ventricular volume overload, or myocardial damage. The features of VR are described to include cell size increases, cardiac fibroblast proliferation, ventricular muscle hypertrophy and cardiac weight increases. Then, VR results in arrhythmia, heart failure or even sudden death; therefore, focusing on how to reverse VR has become an important subject for cardiovascular disease treatment [1].

The pathological process of VR is very complex and involves the sympathetic nervous system (SNS), the renin-angiotensin-aldosterone system (RAAS), inflammatory cytokines, collagen, matrix metalloproteinase and other factors [2–4]. Due to changes in heart function, the levels of angiotensin II (AngII) are increased in VR model rats. AngII can not only induce the occurrence of VR but also spur the secretion of other cytokines though a signalling cascade, such as endothelin 1 (ET-1), aldosterone (ALD), and transforming growth factor-β (TGF-β) [5]. TGF-β is a vital factor that plays a role in accelerating apoptosis by promoting collagen synthesis and inhibiting collagenase release [6]. ET induces cardiomyocyte proliferation, extracellular matrix (ECM) production and vascular remodelling, and its mechanisms include vasoconstriction, neuroendocrine system activation and abnormal gene expression [7,8]. NO is a vasodilating substance and widely participates in various pathophysiological processes, such as the regulation of blood pressure, dilation of blood vessels, inhibition of leukocyte adherence, and prevention of platelet aggregation [9]. NO is catalysed by NO synthase (NOS), which has two isoforms; total NO synthase (tNOS) consists of endothelial NO synthase (eNOS) and inducible NO synthase (iNOS). Reduced eNOS biosynthesis can lead to diastolic function impairment, while iNOS induces endothelial dysfunction [10,11].

Averrhoa carambola L. is classified in the Oxalidaceae family; the fruit is popular with the public for its particular appearance and delicate taste. The *Averrhoa carambola* L. tree is widely cultivated in Asian countries and has been introduced into the Americas, especially Brazil. In Brazil, *Averrhoa carambola* L. has long been welcomed by locals for its excellent effectiveness in suppressing blood glucose and blood

* Corresponding author.
E-mail address: 175072919@qq.com (H. Nong).

https://doi.org/10.1016/j.biopha.2019.109612
Received 5 August 2019; Received in revised form 25 October 2019; Accepted 26 October 2019

pressure elevations; the medicinal portions include the root, stem, leaf and fruit [12]. In addition, *Averrhoa carambola* L. is widely pharmacologically active. Extract from *Averrhoa carambola* L. roots can protect diabetic mice by inhibiting related protein pathways [13] and can protect against pancreatic beta cell dysfunction induced by palmitic acid [14]. Extract from *Averrhoa carambola* L. fruit can be regarded as a prophylactic for hepatocellular carcinoma in mice [15], and extract from *Averrhoa carambola* L. leaves shows considerable anti-inflammatory activity [16]. In addition, the medicinal properties of *Averrhoa carambola* L. also include antioxidant properties [17] as well as properties that alleviate eczema, hangovers, inappetence, headaches, coughing, vomiting and other ailments [15,16]. In China, people use the fruit as a traditional medicine due to its effectiveness in lowering blood pressure and blood lipids, and tests have demonstrated that *Averrhoa carambola* L. can protect rats with diabetic cardiomyopathy [18]. However, whether *Averrhoa carambola* L. can alleviate ventricular remodelling induced by isoprenaline (ISO) remains untested. Thus, we carried out this experiment to investigate this possibility.

2. Materials and methods

2.1. Materials

Tablets of a positive control drug, captopril (Lot No: 20170504), were purchased from Guangdong Taicheng Pharmaceutical Co., Ltd., and dissolved in distilled water to concentration of 5.0 mg/ml. ISO (Lot No: 20170324) was obtained from Shanghai Harvest Pharmaceutical Co., Ltd., and the concentration was adjusted to 0.5 mg/ml with distilled water. NOS detection kits (Lot No: 20170215) were supplied by the Nanjing Jiancheng Bioengineering Institute. TGF-β (Lot No: 201703) and AngII (Lot No: 201701) enzyme-linked immunosorbent assay (ELISA) test kits were procured from Shanghai Hengyuan, Bio-Techne China Co., Ltd. The immunohistochemistry reagents used to detect ET-1 (Lot No: #J1017) and endothelin-converting enzyme (ECE, Lot No: #J1306) were obtained from Santa Cruz Biotechnology. A Masson trichrome staining kit (Lot No: 20170113) was obtained from NanJing JianCheng Bioengineering Institute. Antibodies recognizing TGF-β (Lot No: MA5-15065), ECE (Lot No: MA5-24016), ET-1 (Lot No: MA1-83134), tNOS (Lot No: PA3-032A), iNOS (Lot No: PA1-036), eNOS (Lot No: PA1-037) and polyvinylidene fluoride (PVDF) membrane (Lot No: 88520) were purchased from Thermo Fisher Scientific Inc.

2.2. Herbal preparation

An aqueous extract of *Averrhoa carambola* L. (AEA) was prepared at the Department of Pharmacology, Guangxi Medical University. Fresh *Averrhoa carambola* L. fruit was collected, washed, cut into halves, pitted and weighed, and then an equal volume of distilled water was added to prepare a homogenate. The homogenate was produced with an ultrasonic cell disruptor and stored at 4 °C overnight. The homogenate was separated with a high-speed refrigerated centrifuge for 10 min (8000 g/min). The supernatant was collected and vacuum-concentrated to yield 10 g of raw medicinal material/ml. Then, absolute ethanol was added to this concentrate overnight to obtain the precipitate, which was identified as polysaccharide.

2.3. Animals and treatments

Ventricular remodelling model induced by isoprenaline was widely approved and used [19]. Sixty Sprague-Dawley rats weighing 180 g–220 g (half male and half female) were chosen. The animals were randomly divided into 6 groups (n = 10), housed under standard conditions and given free access to standard rodent chow and water. The groups were as follows:

Normal control group: The rats were given 5 mg/kg/d NS by subcutaneous injection three times a day for 7 days; after the third dose every day, the rats were given 50 mg/kg NS by intragastric administration once a day for 14 days.

Model group: The rats were given 5 mg/kg/d ISO by subcutaneous injection three times a day for 7 days; after the third dose every day, the rats were given 50 mg/kg NS by intragastric administration once a day for 14 days.

Captopril group: The rats were given 5 mg/kg/d ISO by subcutaneous injection three times a day for 7 days; after the third dose every day, the rats were given 50 mg/kg captopril by intragastric administration once a day for 14 days.

AEA_H group: The rats were given 5 mg/kg/d ISO by subcutaneous injection three times a day for 7 days; after the third dose every day, the rats were given 200 mg/kg AEA by intragastric administration once a day for 14 days.

AEA_M group: The rats were given 5 mg/kg/d ISO by subcutaneous injection three times a day for 7 days; after the third dose every day, the rats were given 100 mg/kg AEA by intragastric administration once a day for 14 days.

AEA_L group: The rats were given 5 mg/kg/d ISO by subcutaneous injection three times a day for 7 days; after the third dose every day, the rats were given 50 mg/kg AEA by intragastric administration once a day for 14 days.

All experiments were performed in accordance with approval from the Institutional Animal Care and Use Committee of Guangxi Medical University. Animal ethics review followed the Guiding Opinions on the Treatment of Laboratory Animals issued by the Ministry of Science and Technology of the People's Republic of China and the Laboratory Animal-Guideline for Ethical Review of Animal Welfare issued by the National Standard of the People's Republic of China.

2.4. Examination of the levels of TGF-β and AngII

Twenty-four hours after the last administration, blood samples were collected from the abdominal aorta, and serum was isolated using a refrigerated centrifuge (model number: TDL-5A) with the appropriate parameters (3500 g/min for 10 min, 4 °C). The serum levels of TGF-β and AngII were measured using ELISA kits according to the listed instructions.

2.5. Examination of the levels of tNOS, iNOS and eNOS

Serum samples were isolated and stored at −20 °C. Then, the levels of tNOS, iNOS and eNOS were detected with an NOS typed assay kit; the data for the three types of NOS were obtained simultaneously. The colorimetric method was used with an ultraviolet and visible light spectrophotometer (model number: 722, Shanghai Precision and Scientific Instrument Corporation) under a detection wave length of 530 nm. The experimental procedure was performed in strict accordance with the instructions.

2.6. Determination of the ventricular remodelling index

Before anaesthetization, the rats were weighed, and the data were recorded as body weight (BW) values. After collecting the blood samples, the heart and the kidney were removed from openings in the thoracic cavity and the abdominal cavity, rinsed with pre-cooled normal saline, dried with filter paper, and weighed. The heart weight (HW) and kidney weight (KW) were recorded. The left ventricle was obtained by removing the atrium, vessel, fat, valve and other tissues and then weighed. The weight was recorded as the left ventricle weight (LVW). The ventricular remodelling indexes were calculated as follows:

$$\text{left ventricular index} = (\text{LVW}/\text{BW}) \times 100\%;$$

$$\text{heart index} = (\text{HW}/\text{BW}) \times 100\%; \text{ and}$$

$$\text{kidney index} = (\text{KW}/\text{BW}) \times 100\%.$$

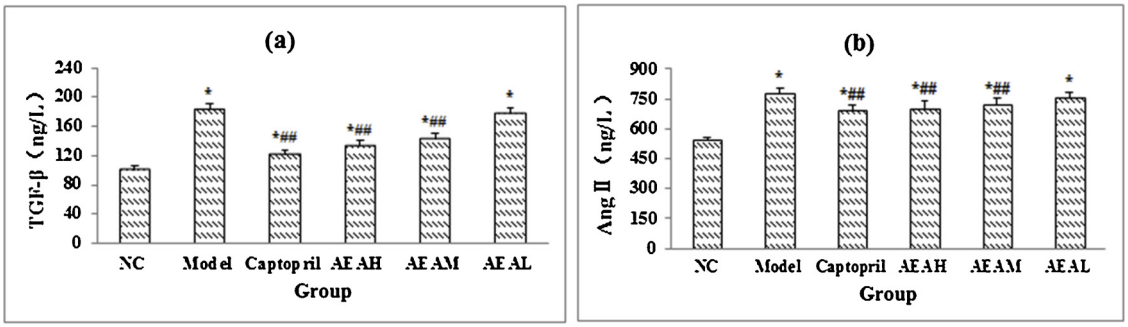

Fig. 1. Effect of AEA on the levels of TGF-β and AngII. Each column represents the mean ± SD. *P < 0.05 compared with the NC group; #P < 0.05 and ##P < 0.01 compared with the model group.

2.7. Immunohistochemical analysis of ECE and ET-1

Left ventricle tissues were prepared, fixed with 10% formalin and embedded in paraffin. The paraffin sections of the left ventricle were deparaffinized, dehydrated, microwave-treated with citrate buffer and washed with PBS. The samples were incubated in H_2O_2 solution (3.0%) to block endogenous peroxidase activity. The sections were then incubated with rabbit polyclonal antibodies against ECE and ET-1 proteins overnight. After they had been washed, the sections were incubated with anti-ECE antibody and anti-ET-1 antibody and then treated with streptavidin-peroxidase and diaminobenzidine. The sections were stained, and the images were acquired with a light microscope (Olympus, Japan). Positive staining was analysed by the optical density (OD) values and calculated by the image analysis software package ImageJ (edition II, developed by the National Institutes of Health).

2.8. Detection of myocardial apoptosis

Paraffin sections of myocardial tissue were used to detect apoptosis by the terminal-deoxynucleotidyl transferase-mediated dUTP nick end Labelling (TUNEL) method. The operating procedure strictly followed to the instructions of the detection kits (Roche). Under the light microscope, normal cardiac myocytes were stained blue, while apoptotic cardiac myocytes were stained sepia in various shades.

2.9. Pathological examination of myocardial tissue

Myocardial tissue was embedded into paraffin blocks to examine pathogenic changes. The paraffin blocks were cut into sections of approximately 5 mm thickness, deparaffinized, dehydrated and stained with haematoxylin and eosin (H&E) according to the manufacturer's instructions. Pathological changes were observed using a light microscope (Olympus, Japan) and were analysed by a researcher who was blinded to the experimental groups.

2.10. Examination of the collagen volume fraction of myocardial tissue

Paraffin sections of the left ventricle were used to determine the collagen volume fraction (CVF) by means of Masson's trichrome staining. The staining results were obtained with light microscopy. Normal tissues were stained red, while fibrotic tissues and surrounding blood vessels were stained blue. The area of the fibrotic tissue was measured using Image-Pro Plus software (IPP, edition VI, developed by Nanjing Dongtu Digital Technology Co., Ltd). CVF was calculated as follows:

CVF = total fibrotic area/total area of the left ventricle

2.11. Western blot analysis for tNOS, eNOS, iNOS, TGF-β, ECE and ET-1

Tissue of left ventricular was fixed in pre-cold RIPA buffer which was added with protease inhibitor. The Left ventricular lysate was obtained and centrifuged (15,000xg at 4 °C for 20 min). The lysate protein samples were quantified and resolved in 10% sodium dodecyl sulfate-polyacrylamide (SDS) gels. Then protein was transferred to PVDF membranes. The membrane was respectively added with the primary polyclonal antibody against tNOS (1:1000), eNOS (1:1000), iNOS (1:1000), TGF-β (1:1000), ECE (1:1000) and ET-1 (1:1000) and incubated overnight at 4 °C. After washed with Tris Buffered Saline Tween (TBST) on a shaker for 3times, the membrane was added with appropriate secondary antibody (1:15,000). Protein bands were scanned using the Q55CW computer image analysis system (Leica, Germany). IOD value of protein bands was calculated by the software of IPP and the level of protein expression was determined with the formula: relative protein level = IOD value of target protein/IOD value of internal control protein x 100%.

2.12. Statistical analysis

SPSS 13.0 software was used to process the data. All the results are presented as the mean ± standard error (SD). The differences between groups were evaluated using the one-way analysis of variance (ANOVA) via the Student–Newman–Keuls post-test. Differences were considered to be significant for P-values < 0.05.

3. Results

3.1. Effect of AEA on the levels of TGF-β and AngII

The ELISA results showed that the serum levels of TGF-β and AngII were increased significantly in the model group compared to the NC group (P < 0.05). The levels of TGF-β and AngII in the captopril group, AEA_H group and AEA_M group were markedly decreased compared with those in the model group (P < 0.01). There were no differences between the AEA_L and model groups (P > 0.05). The results are shown in Fig. 1.

3.2. Effect of AEA on the levels of tNOS, iNOS and eNOS

As shown in Fig. 2, the serum levels of tNOS were decreased in the model group compared with the NC group (P < 0.05). When rats were treated with captopril and AEA, tNOS increased to different levels (P < 0.05 and P < 0.01, respectively), which hinted that administration of AEA could recover the activity of tNOS and the catalysis and production of NO to some extent. Compared with those in the model group, the levels of iNOS were decreased and the levels of eNOS were increased in the groups given captopril and AEA (P < 0.05 and P < 0.01, respectively).

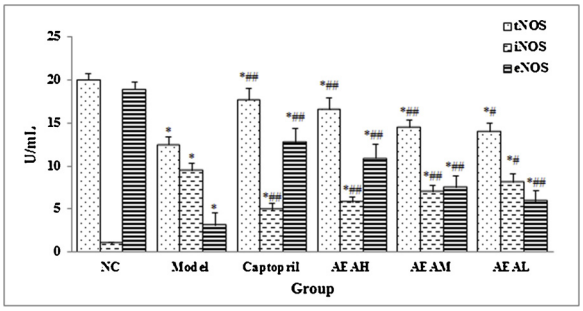

Fig. 2. Effect of AEA on the levels of tNOS, iNOS and eNOS. Each column represents the mean ± SD. *P < 0.05 compared with the NC group; #P < 0.05 and ##P < 0.01 compared with the model group.

3.3. Effect of AEA on the ventricular remodelling index

The left ventricular index (LVW/BW), the heart index (HW/BW) and the kidney index (KW/BW) increased in the model group after ISO administration, which implied that the VR model was successfully established. Rats treated with high doses of captopril and AEA exhibited markedly decreased LVW/BW and HW/BW ratios compared with model rats (P < 0.01), but no differences were observed between rats treated with medium or low doses of AEA and model rats (P > 0.05). The KW/BW ratio was decreased in the groups treated with captopril and AEA (high and medium doses) compared with the model group (P < 0.05 and P < 0.01, respectively). The above experimental results suggest that AEA could ease the progression of VR. The results are shown in Fig. 3.

3.4. Effect of AEA on the protein expression of ECE and ET-1

ECE protein expression increased after injection of ISO in the model group, and administration of captopril and AEA at high doses could effectively lower the positive expression of ECE, suggesting that AEA had the ability to inhibit the activity of ECE. ET-1 protein expression increased due to the overexpression of ECE, causing ET-1 to be catalysed by ECE. High-dose AEA treatment decreased the expression of ET-1 compared to the model treatment (P < 0.05), while medium- and low-dose AEA treatment did not change ET-1 expression compared with the model treatment (P > 0.05). The results are shown in Fig. 4.

3.5. Effect of AEA on myocardial apoptosis

As shown in Fig. 5, the area stained blue presented normal cardiac myocytes, and the area stained sepia presented apoptotic cardiac myocytes. In the model group, the number of apoptotic cardiomyocytes was distinctly increased, while in the NC group, fewer apoptotic cardiomyocytes were observed. When the cardiomyocytes were treated with AEA, the area stained sepia became smaller, and the area stained blue became larger. This result implied that AEA might alleviate VR by inhibiting the apoptosis of cardiomyocytes, thus playing a role in protecting the cardiovascular system.

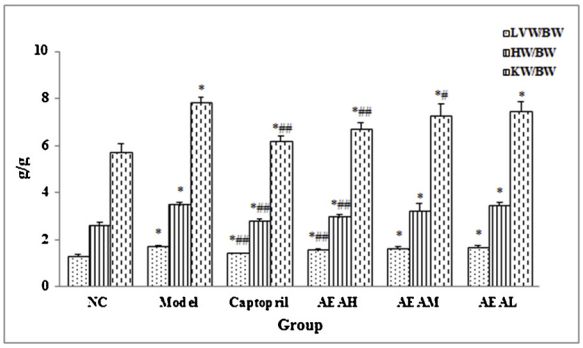

Fig. 3. Effect of AEA on the ventricular remodelling index. Each column represents the mean ± SD. The left ventricular index, heart index and kidney index are respectively presented as LVW/BW, HW/BW and KW/BW. *P < 0.05 compared with the NC group; #P < 0.05 and ##P < 0.01 compared with the model group.

3.6. Effect of AEA on pathological changes

Pathological changes in myocardial tissue were examined with the method of H&E staining. As shown in Fig. 6, large areas of necrosis and inflammatory cell infiltration were visible along with widening of the space between cardiac fibroblasts and loss of cardiomyocyte structures in the model group. In the group treated with AEA, the necrosis was clearly reduced and had become diffuse. In addition, alleviation of interstitial oedema and reductions in monocyte infiltration were observed in the captopril group and the AEA_H group.

3.7. Effect of AEA on the collagen volume fraction of myocardial tissue

The collagen volume fraction (CVF) was measured by Masson's trichrome staining. Normal tissues were stained red, fibrotic tissues were stained blue, and collagen was distinguishable from muscle tissue. As shown in Fig. 7, there was substantial collagen exposure and CVF was increased in the model group compared with the NC group (P < 0.05). After administration of AEA, collagen exposure was reduced and the CVF value was decreased in the AEA-treated group compared with the model group (p < 0.01). There was no difference between the AEA_L group and the model group (P > 0.05).

3.8. Effect of AEA on the protein expression of tNOS, eNOS, iNOS, TGF-β, ECE and ET-1

As shown in Fig. 8, the protein expression of tNOS was decreased in the model group compared with the NC group (P < 0.05). When rats were treated with captopril and AEA, tNOS increased to different levels (P < 0.05 and P < 0.01, respectively), which hinted that administration of AEA could recover the activity of tNOS and the catalysis and production of NO to some extent. Compared with those in the model group, the levels of iNOS were decreased and the levels of eNOS were increased in the groups given captopril and AEA (P < 0.05 and P < 0.01, respectively). The protein expression of TGF-β, ECE and ET-1 were increased in the model group compared with the NC group (P < 0.05). When rats were treated with captopril and AEA, levels of TGF-β, ECE and ET-1 decreased to different levels (P < 0.05 and P < 0.01, respectively).

4. Discussion

Injection of ISO has long been used to establish VR models, but the mechanism has remained uncertain. In 1959, an investigation pointed out that myocardial tissue subjected to prolonged exposure to a β-receptor agonist was more likely to die than non-exposed tissue [19]. The mechanisms might include the following: on the one hand, the increase in myocardial oxygen consumption could have led to ischaemia, anoxia and necrosis of cardiomyocytes, generating compensatory heart hypertrophy, collagen proliferation, collagen scarring and heart function decline; on the other hand, cyclic adenosine monophosphate (cAMP) may have been activated by the excess ISO, leading to excitement of sympathetic nerves, elevations in heart rate, increases in pressure load, hypertrophy of cardiac myocytes and remodelling of ventricles. In the present study, we found that heart weight and left ventricular weight were increased and that apoptosis, fibrosis, necrosis and inflammatory infiltration were visible after treatment with excess ISO, which reflected that the VR model was successfully established.

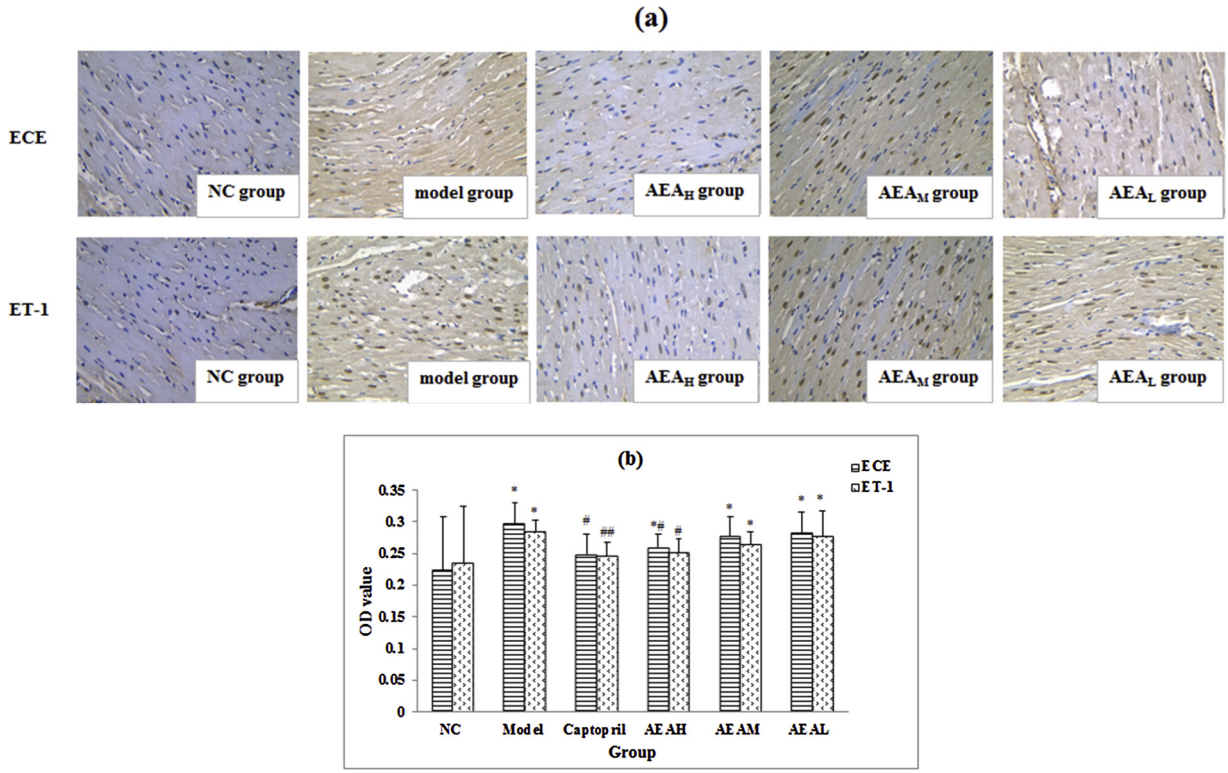

Fig. 4. Effect of AEA on the protein expression of ECE and ET-1. The tissue samples were subjected to immunohistochemical analysis and observed under a light microscope at 400× magnification. Positive expression is indicated by a sepia colour.
Each column represents the mean ± SD. *P < 0.05 compared with the NC group; $^{\#}$P < 0.05 and $^{\#\#}$P < 0.01 compared with the model group.

Serum biomarkers of endothelial dysfunction include TGF-β, AngII, NOS, NO, ECE, and ET [10]. There are several possible mechanisms of TGF-β participation in VR, as follows: 1). TGF-β enhances the mRNA expression and synthesis of fibrillar collagen types I and III [20]; 2). TGF-β is associated with tissue repair and fibrosis [21]; and 3). TGF-β increases the accumulation of fibrous protein, collagen and proteoglycan by upregulating the expression and inhibiting the degradation of ECM [22]. Thus, TGF-β is regarded as the common pathway of VR induced by various factors. In this study, we found that AEA was able to downregulate the level of TGF-β, which implied that the decrease in the collagen volume fraction was associated with the low content of TGF-β to some degree.

Early in 1988 [23], Japanese scientists isolated and purified a small-molecule polypeptide from porcine aortic endothelial cells; this bioactive substance was called endothelin (ET). ET is a potent vasoconstrictor and exists in three isoforms, ET-1, ET-2 and ET-3; ET-1 shows the highest vasoconstrictive activity. ET accelerates the abnormal growth of cardiomyocytes and fibroblasts, which leads to collagen

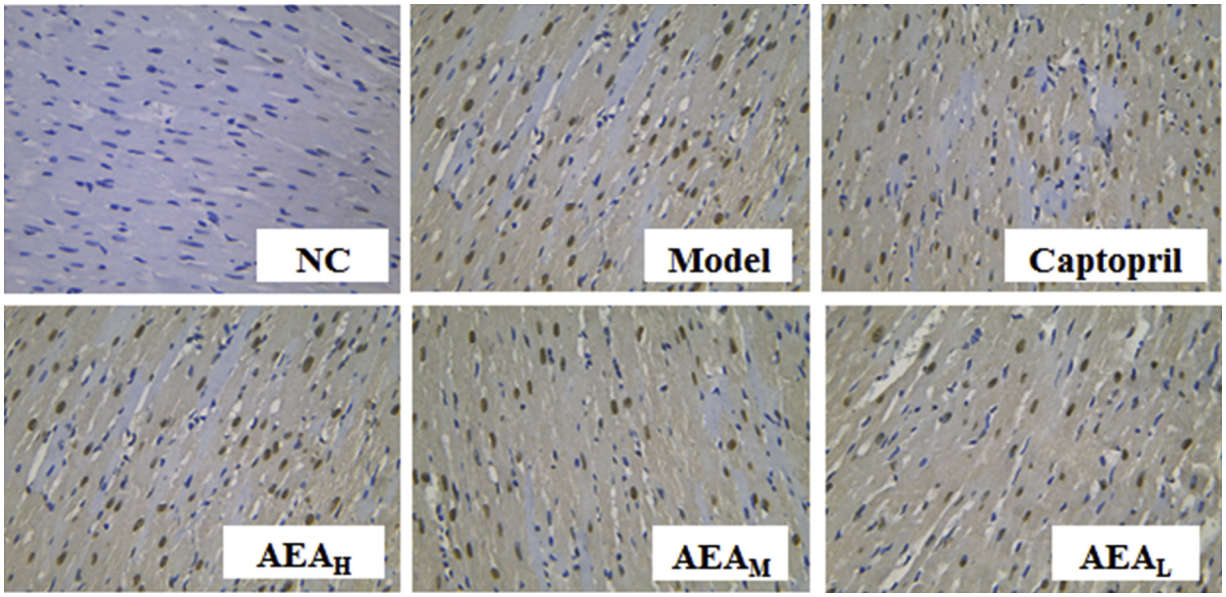

Fig. 5. Effect of AEA on myocardial apoptosis. The tissue samples were analysed by the TUNEL method and observed under a light microscope with a magnification of 400×. Normal cardiac myocytes are stained blue, while apoptotic cardiac myocytes are stained sepia of various shades.

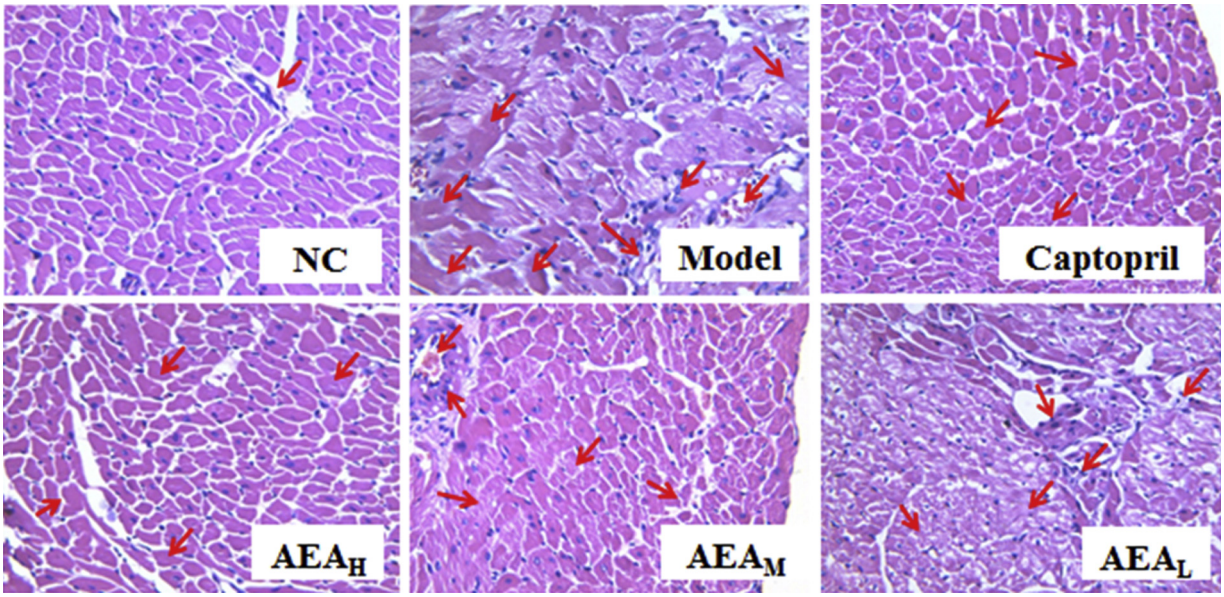

Fig. 6. Effect of AEA on pathological changes. The sections were observed under a light microscope at 400× magnification. In the model group, necrosis was widely distributed, and necrotic areas were fused together; in the AEA_H group and the captopril group, the above situation was alleviated.

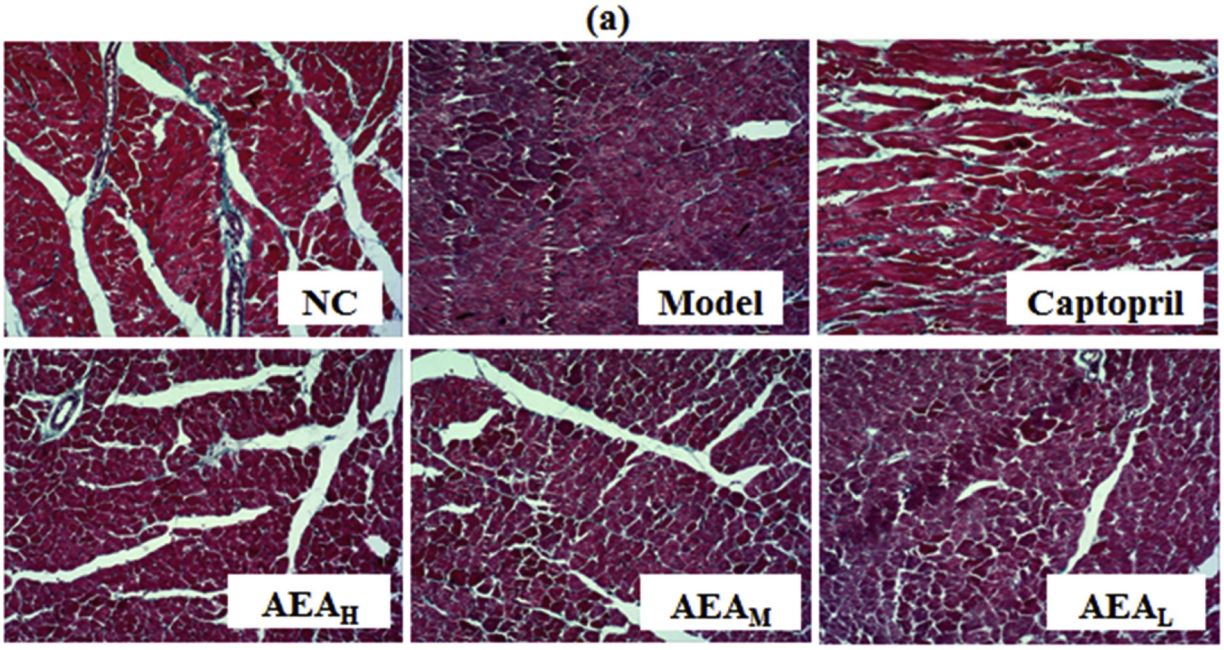

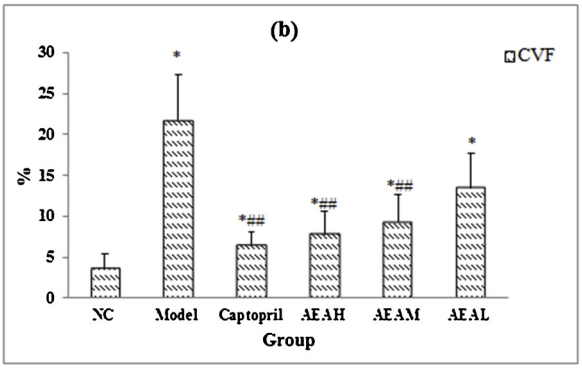

Fig. 7. Effect of AEA on the collagen volume fraction of myocardial tissue (400x). CVF (%) was used to estimate the condition of collagen exposure and the degree of myocardial fibrosis.

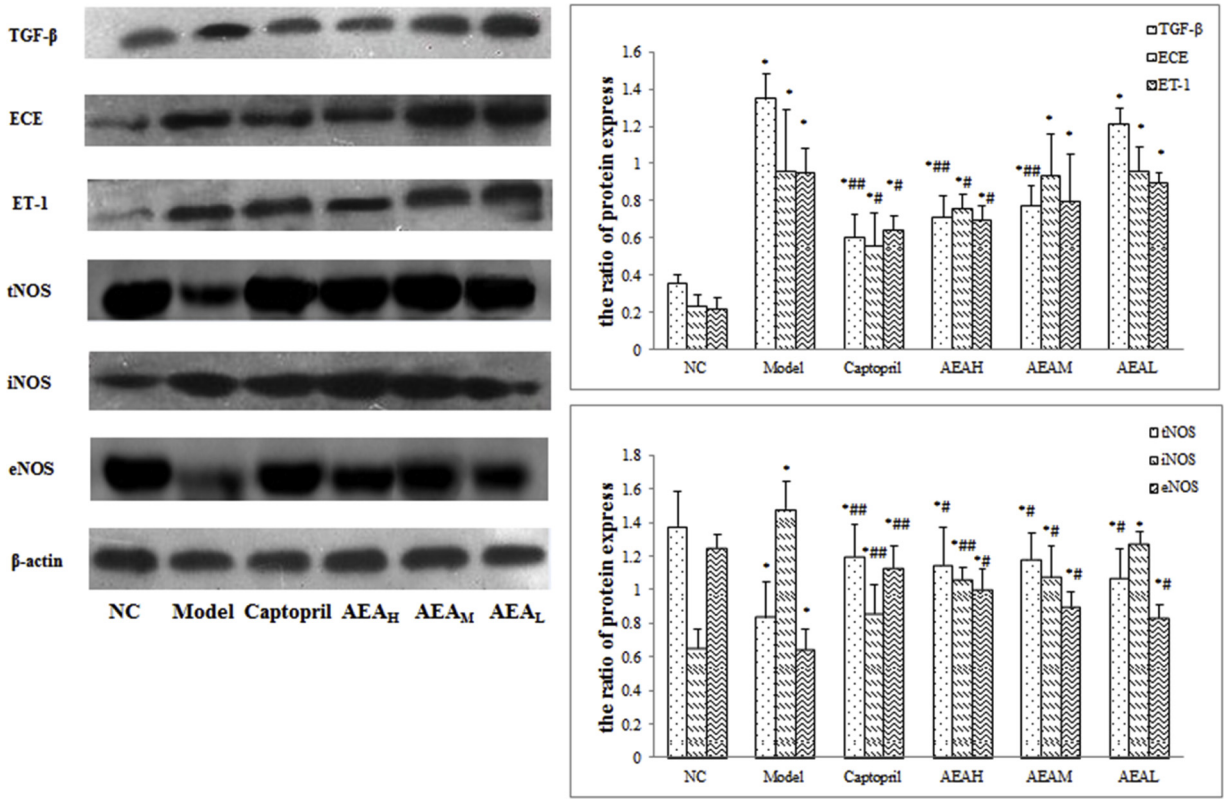

Fig. 8. Effect of AEA on the protein expression of tNOS, eNOS, iNOS, TGF-β, ECE and ET-1. The level change of the protein was detected by Western blot. Each column represents the mean ± SD. *P < 0.05 compared with the NC group; #P < 0.05 and ##P < 0.01 compared with the model group.

deposition, blood vessel wall thickening and vessel wall shortening and stiffening. Investigations have verified that the levels of ET-1 increase during acute myocardial infarction, endothelial injury, myocardial anoxia, atherosclerosis, heart failure and other conditions [24–26]. The results of our research showed elevated ET-1 levels, which were consistent with the above results of previous studies.

Pro-ET was catalysed to ET by endothelin-converting enzyme (ECE), and we found that AEA had the potential to weaken the activity of ECE. Moreover, ECE had the capacity to promote the conversion from AngI to AngII, as reported by Wada [27]. Similarly, inhibiting the activity of ECE can reduce the secretion of AngII [28]. This implies that ECE might be regarded as a target for drug research for VR. AngII is widely known for its bioactivity causing vasoconstriction. Overexpression of AngII initiates endothelial dysfunction [29], lipid peroxidation [30] and vascular inflammation [31]. The hypothesis that AEA lowers the levels of AngII by reducing the activity of ECE was confirmed because in the model group, the content of AngII was higher than that in other groups treated with positive control drug and AEA.

In the present study, we found that the level of iNOS decreased while the level of eNOS increased after administration of AEA. In general, the expression of iNOS is very low, but when myocardial ischaemia, myocardial anoxia, inflammatory reactions and cytokine stimulation occur, the activity of iNOS increases. Then, cytotoxicity and cardiomegaly are mediated by the overexpression of iNOS [32,33]. eNOS is beneficial for the cardiovascular system and can reverse myocardial hypertrophy [34]; once the balance of eNOS levels is disrupted, dysfunction of myocardial contraction and relaxation occurs [35].

5. Conclusions

In conclusion, the study used a model of VR induced by ISO to explore the effect of AEA on the function of the vascular endothelium. The present results demonstrated that AEA lowered the levels of TGF-β, AngII, iNOS, ECE, and ET-1 and decreased the ventricular remodelling index and CVF. The activity of tNOS and eNOS was elevated by AEA treatment. Lesions were attenuated and collagenous tissue was reduced by AEA treatment, as detected by H&E staining and Masson's trichrome staining, respectively. The above results might partly suggest the protective effect of AEA, and AEA-mediated alleviation of VR in rats might be related to maintenance of the balance of vasoactive substances and the function of the vascular endothelium.

6. Study limitations

However, many reports have suggested that there are side effects of star fruit. Uraemic patients have shown symptoms such as hiccups and vomiting after taking star fruit [36]. Patients with renal failure who have ingested this fruit have also suffered neurological symptoms [37]. So far, we have been alerted that there exist dual effects during the use of *Averrhoa carambola* L., and the protective effects and the side effects needed to be studied more thoroughly. In addition, the cardiovascular protective of an aqueous extract of *Averrhoa carambola* L. is only a basic research, and AEA is only a polysaccharide but not a monomer. AEA is gained according to the operation of "2.2Herbal preparation" with high purity (a single narrow symmetrical peak was gained though Sephadex g-100 column chromatography). Furthermore, we have firstly gained a monomer named 2-dodecyl-6-methoxycyclohexa-2,5-diene-1, 4-dione which is isolated from *Averrhoa carambola* L., and we intend to use the highly reactive monomer to carry out deeper research in the future based on this research.

Contributions

Xingmei Liang and Huiliang Nong wrote the main manuscript text, Renbin Huang and Jianchun Huang prepared the figures, Chunxia Chen

and Feizhang Qin searched the references, Antao Liu and Xiaojun Tang performed the experiments and Tian Ning analysed the experimental data.

Data availability

All data generated or analysed during this study are included in this published article.

Declaration of Competing Interest

The authors declare that there are no conflicts of interest.

Acknowledgement

These authors gratefully acknowledge financial support from the Project of Higher Education in Guangxi Department of Education to Enhance the Basic Capacity of Young Teachers [grant number: 2017KY1227] and Guangxi Vocational Education Program for Pharmacy Major Developing and Researching Base [grant number: Vocational Education in Guangxi 2018-65].

References

[1] J.E. Udelson, M.A. Konstam, Ventricular remodeling fundamental to the progression (and regression) of heart failure, J. Am. Coll. Cardiol. 57 (March (13)) (2011) 1477–1479.
[2] E.N. Amosova, Y.V. Shpak, A.V. Nedozhdij, L.V. Produsevich, Proinflammatory cytokine levels in patients with diastolic heart failure, Kardiol. Pol. 61 (July (7)) (2004) 17–20.
[3] A.M. Candia, H. Villacorta Jr., E.T. Mesquita, Immune-inflammatory activation in heart failure, Arq. Bras. Cardiol. 89 (September (3)) (2007) 183–190 201-208.
[4] A. Diwan, Z. Dibbs, S. Nemoto, G. DeFreitas, B.A. Carabello, N. Sivasubramanian, E.M. Wilson, F.G. Spinale, D.L. Mann, Targeted overexpression of noncleavable and secreted forms of tumor necrosis factor provokes disparate cardiac phenotypes, Circulation 109 (January (2)) (2004) 262–268.
[5] K. Tokuda, H. Kai, F. Kuwahara, H. Yasukawa, N. Tahara, H. Kudo, K. Takemiya, M. Koga, T. Yamamoto, T. Imaizumi, Pressure-independent effects of angiotensin II on hypertensive myocardial fibrosis, Hypertension 43 (February (2)) (2004) 499–503.
[6] C. Laviades, N. Varo, J. Díez, Transforming growth factor beta in hypertensives with cardiorenal damage, Hypertension. 36 (October (4)) (2000) 517–522.
[7] T. Emori, Y. Hirata, K. Ohta, M. Shichiri, F. Marumo, Secretory mechanism of immunoreactive endothelin in cultured bovine endothelial cells, Biochem. Biophys. Res. Commun. 160 (April (1)) (1989) 93–100.
[8] H. Fujisaki, H. Ito, Y. Hirata, M. Tanaka, M. Hata, M. Lin, S. Adachi, H. Akimoto, F. Marumo, M. Hiroe, Natriuretic peptides inhibit angiotensin II-induced proliferation of rat cardiac fibroblasts by blocking endothelin-1 gene expression, J. Clin. Invest. 96 (August (2)) (1995) 1059–1065.
[9] S.M. Nadtochiy, L.S. Burwell, P.S. Brookes, Cardioprotection and mitochondrial S-nitrosation: effects of S-nitroso-2-mercaptopropionyl glycine (SNO-MPG) in cardiac ischemia-reperfusion injury, J. Mol. Cell. Cardiol. 42 (April (4)) (2007) 812–825.
[10] D.H. Endemann, E.L. Schiffrin, Endothelial dysfunction, JASN 15 (August (8)) (2004) 1983–1992.
[11] A. Warnholtz, M.A. Ostad, T. Heitzer, B.U. Goldmann, G. Nowak, T. Munzel, Effect of tirofiban on percutaneous coronary intervention-induced endothelial dysfunction in patients with stable coronary artery disease, Am. J. Cardiol. 95 (January (1)) (2005) 20–23.
[12] R. Soncini, M.B. Santiago, L. Orlandi, G.O. Moraes, A.L. Peloso, M.H. dos Santos, G. Alves-da-Silva, V.A. Paffaro Jr., A.C. Bento, A. Giusti-Paiva, Hypotensive effect of aqueous extract of Averrhoa carambola L. (Oxalidaceae) in rats: an in vivo and in vitro approach, J. Ethnopharmacol. 133 (January (2)) (2011) 353–357.
[13] X. Xu, T. Liang, X. Lin, Q. Wen, X. Liang, W. Li, F. Qin, N. Zheng, J. Ming, R. Huang, Effect of the total extract of averrhoacarambola (Oxalidaceae) root on the expression levels of TLR4 and NF-κB in streptozotocin-induced diabetic mice, Cell. Physiol. Biochem. 36 (6) (2015) 2307–2316.
[14] Q. Xie, S. Zhang, C. Chen, J. Li, X. Wei, X. Xu, F. Xuan, N. Chen, T. Pham, N. Qin, J. He, F. Ye, W. Huang, R. Huang, Q. Wen, Protective effect of 2-dodecyl-6-methoxycyclohexa-2, 5-diene-1, 4-dione, isolated from Averrhoa carambola L., against palmitic acid-induced inflammation and apoptosis in Min6 cells by inhibiting the TLR4-MyD88-NF-κB signaling pathway, Cell. Physiol. Biochem. 39 (5) (2016) 1705–1715.
[15] R. Singh, J. Sharma, P.K. Goyal, Prophylactic role of Averrhoa carambola (Star fruit) extract against chemically induced hepatocellular carcinoma in swiss albino mice, Adv. Pharmacol. Sci. 2014 (2014) 158936.
[16] D.A. Cabrini, H.H. Moresco, P. Imazu, C.D. da Silva, E.F. Pietrovski, D.A. Mendes, A. da Silveira Prudente, M.G. Pizzolatti, I.M. Brighente, M.F. Otuki, Analysis of the potential topical anti-inflammatory activity of Averrhoa carambola L. in mice, Evid. Complement. Alternat. Med. 2011 (2011) 908059.
[17] S. Saikia, N.K. Mahnot, C.L. Mahanta, A comparative study on the effect of conventional thermal pasteurisation, microwave and ultrasound treatments on the antioxidant activity of five fruit juices, Food Sci. Technol. Int. 22 (June (4)) (2016) 288–301.
[18] W.S. Li, F. Fang, F.Z. Qin, R.B. Huang, Y. Jiao, Effects of Averrhoa carambola root extract on diabetic cardiomyopathy in rats, Chin. J. Exp. Tradit. Med. Formulae 21 (7) (2015) 128–132.
[19] G. Rona, Ci Chappel, T. Balazs, R. Gaudry, An infarct-like myocardial lesion and other toxic manifestations produced by isoproterenol in the rat, AMA Arch. Pathol. 67 (April (4)) (1959) 443–455.
[20] M. Eghbali, R. Tomek, V.P. Sukhatme, C. Woods, B. Bhambi, Differential effects of transforming growth factor-beta 1 and phorbol myristate acetate on cardiac fibroblasts. Regulation of fibrillar collagen mRNAs and expression of early transcription factors, Circ. Res. 69 (August (2)) (1991) 483–490.
[21] T. Brand, M.D. Schneider, The TGF beta superfamily in myocardium: ligands, receptors, transduction, and function, J. Mol. Cell. Cardiol. 27 (January (1)) (1995) 5–18.
[22] G. Yu, X. Liang, X. Xie, T. Yang, M. Sun, S. Zhao, Apoptosis, myocardial fibrosis and angiotensin II in the left ventricle of hypertensive rats treated with fosinopril or losartan, Chin. Med. J. (Engl.). 115 (September (9)) (2002) 1287–1291.
[23] M. Yanagisawa, H. Kurihara, S. Kimura, Y. Tomobe, M. Kobayashi, Y. Mitsui, Y. Yazaki, K. Goto, T. Masaki, A novel potent vasoconstrictor peptide produced by vascular endothelial cells, Nature 332 (March (6163)) (1988) 411–415.
[24] A. Lerman, B.S. Edwards, J.W. Hallett, D.M. Heublein, S.M. Sandberg, J.C.Jr. Burnett, Circulating and tissue endothelin immunoreactivity in advanced atherosclerosis, N. Engl. J. Med. 325 (October (14)) (1991) 997–1001.
[25] D.J. Stewart, G. Kubac, K.B. Costello, P. Cernacek, Increased plasma endothelin-1 in the early hours of acute myocardial infarction, J. Am. Coll. Cardiol. 18 (July (1)) (1991) 38–43.
[26] R. Pacher, B. Stanek, M. Hülsmann, J. Koller-Strametz, R. Berger, M. Schuller, E. Hartter, E. Ogris, B. Frey, G. Heinz, G. Maurer, Prognostic impact of big endothelin-1 plasma concentrations compared with invasive hemodynamic evaluation in severe heart failure, J. Am. Coll. Cardiol. 27 (March (3)) (1996) 633–641.
[27] A. Wada, T. Tsutamoto, M. Ohnishi, M. Sawaki, D. Fukai, Y. Maeda, M. Kinoshita, Effects of a specific endothelin-converting enzyme inhibitor on cardiac, renal, and neurohumoral functions in congestive heart failure: comparison of effects with those of endothelin A receptor antagonism, Circulation 99 (February (4)) (1999) 570–577.
[28] D.N. Muller, A. Mullally, R. Dechend, J.K. Park, A. Fiebeler, B. Pilz, B.M. Löffler, D. Blum-Kaelin, S. Masur, H. Dehmlow, J.D. Aebi, H. Haller, F.C. Luft, Endothelin-converting enzyme inhibition ameliorates angiotensin II-induced cardiac damage, Hypertension 40 (December (6)) (2002) 840–846.
[29] Q.N. Diep, F. Amiri, R.M. Touyz, J.S. Cohn, D. Endemann, M.F. Neves, E.L. Schiffrin, PPARalpha activator effects on Ang II-induced vascular oxidative stress and inflammation, Hypertension 40 (December (6)) (2002) 866–871.
[30] R.M. Touyz, E.L. Schiffrin, Ang II-stimulated superoxide production is mediated via phospholipase D in human vascular smooth muscle cells, Hypertension 34 (October (4 Pt 2)) (1999) 976–982.
[31] E.L. Schiffrin, R.M. Touyz, Multiple actions of angiotensin II in hypertension: benefits of AT1 receptor blockade, J. Am. Coll. Cardiol. 42 (September (5)) (2003) 911–913.
[32] P.F. Mount, B.E. Kemp, D.A. Power, Regulation of endothelial and myocardial NO synthesis by multi-site eNOS phosphorylation, J. Mol. Cell. Cardiol. 42 (February (2)) (2007) 271–279.
[33] Y. Sun, O.A. Carretero, J. Xu, N.E. Rhaleb, F. Wang, C. Lin, J.J. Yang, P.J. Pagano, X.P. Yang, Lack of inducible NO synthase reduces oxidative stress and enhances cardiac response to isoproterenol in mice with deoxycorticosterone acetate-salt hypertension, Hypertension 46 (December (6)) (2005) 1355–1361.
[34] M. Ozaki, S. Kawashima, T. Yamashita, T. Hirase, Y. Ohashi, N. Inoue, K. Hirata, M. Yokoyama, Overexpression of endothelial nitric oxide synthase attenuates cardiac hypertrophy induced by chronic isoproterenol infusion, Circ. J. 66 (September (9)) (2002) 851–856.
[35] P.B. Massion, J.L. Balligand, Modulation of cardiac contraction, relaxation and rate by the endothelial nitric oxide synthase (eNOS): lessons from genetically modified mice, J. Physiol. 546 (January (Pt 1)) (2003) 63–75.
[36] M.M. Neto, J.A. da Costa, N. Garcia-Cairasco, J.C. Netto, B. Nakagawa, M. Dantas, Intoxication by star fruit (Averrhoa carambola) in 32 uraemic patients: treatment and outcome, Nephrol. Dial. Transplant. 18 (January (1)) (2003) 120–125.
[37] J.M. Chang, S.J. Hwang, H.T. Kuo, J.C. Tsai, J.Y. Guh, H.C. Chen, J.H. Tsai, Y.H. Lai, Fatal outcome after ingestion of star fruit (Averrhoa carambola) in uremic patients, Am. J. Kidney Dis. 35 (February (2)) (2000) 189–193.